


Unsupervised Data-Driven Classification of Topological Gapped Systems with Symmetries

Yang Long¹ and Baile Zhang^{1,2,*}¹*Division of Physics and Applied Physics, School of Physical and Mathematical Sciences, Nanyang Technological University, Singapore 637371, Singapore*²*Centre for Disruptive Photonic Technologies, Nanyang Technological University, Singapore 637371, Singapore* (Received 11 May 2022; revised 18 November 2022; accepted 20 December 2022; published 18 January 2023)

A remarkable breakthrough in topological phase classification is the establishment of the topological periodic table, which is mainly based on the classifying space analysis or K theory, but not based on concrete Hamiltonians that possess finite bands or arise in a lattice. As a result, it is still difficult to identify the topological phase of an arbitrary Hamiltonian; the common practice is, instead, to check the incomplete and still growing list of topological invariants one by one, very often by trial and error. Here, we develop unsupervised classifications of topological gapped systems with symmetries, and demonstrate the data-driven construction of the topological periodic table without *a priori* knowledge of topological invariants. This unsupervised data-driven strategy can take into account spatial symmetries, and further classify phases that were previously classified as trivial in the past. Our Letter introduces machine learning into topological phase classification and paves the way for intelligent explorations of new phases of topological matter.

DOI: [10.1103/PhysRevLett.130.036601](https://doi.org/10.1103/PhysRevLett.130.036601)

Topological systems exhibit topological properties and phenomena [1–4]. The interplay between symmetry and topology plays an important role in symmetry-protected topological phases [5–8]. As a remarkable breakthrough, the establishment of the topological periodic table has revealed the fundamental principles and hidden periodic patterns in symmetry-protected topological phases [5–7,9]. Just like the periodic table of elements in chemistry, the topological periodic table serves as a roadmap in the exploration of new topological materials and topological phases under symmetries.

The topological periodic table is established mainly based on the homotopy group properties of classifying spaces for general Hamiltonians or K theory [6,7,9]. However, its application suffers from some limitations as follows: (1) It is difficult to judge whether an arbitrary Hamiltonian under a given symmetry is topological or not, because the topological periodic table is not derived from analyzing specific Hamiltonians that possess finite bands or arise in a lattice. (2) Some phases that were considered trivial in the past have been found to carry topological properties, e.g., the valley Hall phase [10] and higher-order topological phase [11]. (3) Defining topological invariants in high dimensions (i.e., $d \geq 4$, d is the dimension) is still difficult. Besides the above limitations, to identify the topological phase of a concrete Hamiltonian, one needs to check the list of existing topological invariants one-by-one, very often by trial and error. However, the list of topological invariants is incomplete and still growing. Hence, it is desirable to identify topological phases without relying on the limited knowledge of topological invariants.

Recently, machine learning has been introduced into physical research as a powerful tool for data analysis [12–17], e.g., the deep-learning-enhanced image construction [18–20], the functional optical device engineering [21–27], and the inverse design of topological photonic insulators [28–30]. Many applications of machine learning in physics usually require extensive data with well-defined labels; they belong to so-called supervised learning, and may fail to find new labels beyond *a priori* knowledge. Unsupervised learning, which aims to capture hidden features from raw data without *a priori* human knowledge, has attracted a lot of attention in phase identification in many-body systems [31–33], band topology detection [34–38], and the learning of non-Hermitian systems [39]. Thus, unsupervised learning can be a powerful approach toward topological phase classification under given symmetries without suffering from the above limitations of the topological periodic table.

In this Letter, we demonstrate the unsupervised classification of topological gapped systems with symmetries and the data-driven construction of the topological periodic table, without the mathematical knowledge of group theory or *a priori* topological invariants. Based on the intuitive picture of topology, we propose a similarity function to measure the topological difference between two samples of Hamiltonians. With this similarity function, we perform our proposed clustering algorithm to find the number of topologically different phases automatically. By exploiting randomly generated Hamiltonian samples under different symmetry conditions, the topological periodic table is generated unsupervisedly, with extra information revealed

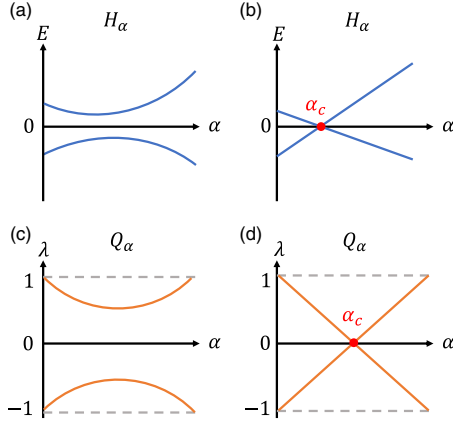


FIG. 1. Band topology for gapped Hamiltonians under symmetries. During continuous deformations from $\alpha = 0$ to $\alpha = 1$, the $H_\alpha = (1 - \alpha)H_1 + \alpha H_2$ will (a) not close the gap if H_1 and H_2 are topologically equivalent, or (b) close the gap when they are topologically distinct. The existence of the band closing point α_c is responsible for determining the topological classification, but α_c is not fixed, due to the arbitrary eigenvalues E of H_1 and H_2 . With the flattened Hamiltonians Q_1 and Q_2 , the $Q_\alpha = (1 - \alpha)Q_1 + \alpha Q_2$ will (c) not close, or (d) close the gap, being consistent with the topological properties of H_1 and H_2 . However, here α_c for Q_α is a constant: $\alpha_c = 1/2$.

about the relation between the number of topological phases and the number of bands. Finally, we also demonstrate the topological classification of phases based on spatially rotational symmetries C_3 and C_4 .

Intuitively, two gapped quantum Hermitian systems H_1 and H_2 under the same symmetry are topologically equivalent if their Hamiltonians can be continuously deformed into each other without ever closing the energy gap. The continuous deformation can be defined as $H_\alpha = (1 - \alpha)H_1 + \alpha H_2$, $\alpha \in [0, 1]$. To demonstrate the concept of topological classification, we consider that H_1 and H_2 are two two-band Hamiltonians here. We illustrate the two possible cases for H_α in Figs. 1(a) and 1(b), showing that H_1 and H_2 are (a) topologically equivalent if there is no energy crossing point, and (b) topologically distinct if there is an energy crossing point α_c whose existence is robust against perturbations. Note that sometimes in case (a), there might be an “accidental” crossing point, but it can be easily removed by perturbations [40]. It should be stressed that the topological phases discussed in this Letter are protected by symmetries. There can be topological phase transitions without gap closing, if the symmetry conditions are changed [51,52], but such changes violate the concept of continuous deformation due to the discrete nature of symmetries.

According to the above analysis, the existence of α_c can be core evidence for classifying the topological gapped systems. However, as shown in Fig. 1(b), the value of α_c is not fixed due to the arbitrary eigenvalues of Hamiltonians. Here, we show an equivalent representation of H_α with

constant α_c . For a Hamiltonian H , one can obtain the eigenequation $H|\psi_{m,k}\rangle = E_m|\psi_{m,k}\rangle$ and $H^\dagger|\varphi_{m,k}\rangle = E_m|\varphi_{m,k}\rangle$, where m denotes the m th band and \mathbf{k} is the wave vector. The projection operator can be defined as $P(\mathbf{k}) = \sum_{m \in \text{occ}} |\psi_{m,k}\rangle \langle \varphi_{m,k}|$, where occ means the occupied bands, namely $\text{occ} = \{m | E_m < E_f\}$. It has been shown that $P(\mathbf{k})$ can be used in topological classifications [34,53–55]. Here we consider the Fermi level as $E_f = 0$. As an equivalent representation, we can define a flattened Hamiltonian as $Q(\mathbf{k}) = 1 - 2P(\mathbf{k})$ [5,56], which has the eigenvalues as ± 1 . This Q plays a role similar to H , carrying the essential information of H [7]. As shown in Figs. 1(c) and 1(d), the eigenvalue λ of $Q_\alpha = (1 - \alpha)Q_1 + \alpha Q_2$ has a crossing point with $\lambda = 0$ (i.e., Fermi level) at the constant point $\alpha_c = 1/2$ if H_1 and H_2 are topologically distinct. The reason for $\alpha_c = 1/2$ is the linear dependence of the crossing eigenvalue branches on α in a topological transition with continuous deformation [40]. For Hamiltonians in more than zero dimensions, the scenarios in Fig. 1(d) can occur at the momenta that exhibit the topological gap closing, whereas the continuous deformation of Q will still resemble the case in Fig. 1(c) at all other momenta. For the Hamiltonians H_i and H_j , $Q_i(\mathbf{k}) + Q_j(\mathbf{k}) = 2Q_{\alpha_c}$, where Q_i is the flattened Hamiltonian of H_i . Based on the above analysis, we propose a similarity function \mathcal{K}_{ij} between the Hamiltonians H_i and H_j as

$$\mathcal{K}_{ij} = \prod_{\mathbf{k} \in \text{BZ}} \left(1 - e^{-\frac{|\det[Q_i(\mathbf{k}) + Q_j(\mathbf{k})]|^2}{\varepsilon^2}} \right) \quad (1)$$

where $\mathcal{K}_{ij} \in [0, 1]$, ε is a constant, and BZ means the Brillouin zone. Obviously, $\mathcal{K}_{ij} = 0$ when H_i and H_j are topologically distinct since one of the eigenvalues is zero, and $\mathcal{K}_{ij} \neq 0$ when they are topologically equivalent. For practical computation, we assume $\varepsilon \rightarrow 0$ so that \mathcal{K}_{ij} can be approximately treated as a binary step function [40]: $\mathcal{K}_{ij} = 1$ when H_i and H_j are topologically equivalent, and $\mathcal{K}_{ij} = 0$ otherwise. The robustness of the crossing point is sufficient to manifest topologically distinct phases. There are two mechanisms in our algorithm to guarantee the accuracy of topological phase identification: (1) the random generation of Hamiltonian samples and (2) the introduction of symmetry-preserved perturbations in the similarity function [40].

After obtaining the similarities between Hamiltonians, we perform our proposed clustering algorithm to figure out how many topologically distinct phases the Hamiltonian samples $\{H_i\}$ under given symmetries can have. In our algorithm, there are a set \mathcal{S} and a list $\{M_c\}$: $\mathcal{S} = \{H_{p_c}\}$ is a set of samples that are mutually different (i.e., $\mathcal{K}_{p_c p_{c'}} < \kappa_c$, $\forall H_{p_c}, H_{p_{c'}} \in \mathcal{S}$, $\kappa_c = 1/2$ is the center value of the value range of \mathcal{K}_{ij}) and M_c denotes the number of samples that

are topologically equivalent to H_{p_c} , $\{M_c | c = 1, 2, \dots, N_c\}$. Our proposed algorithm contains the two steps: (1) Add the first sample H_1 into \mathcal{S} since the initial $\mathcal{S} = \emptyset$. Then, $\mathcal{S} = \{H_1\}$, $p_1 = 1$, $M_1 = 1$, and $N_c = 1$. (2) Compare the following sample H_j with the samples in \mathcal{S} : if H_j is topologically equivalent to H_{p_c} , i.e., $H_{p_c} \in \mathcal{S}$ and $\mathcal{K}_{j,p_c} > \kappa_c$, then $M_c := M_c + 1$. Otherwise, if none of the samples in \mathcal{S} is topologically equivalent to H_j , we add H_j into \mathcal{S} , $M_{N_c+1} = 1$, $p_{N_c+1} = j$, and $N_c := N_c + 1$. After calculating all samples in $\{H_i\}$, we can obtain the following: N_c denotes the number of topologically distinct phases, and $\{M_c\}$ denotes the number of samples that have the same phase as H_{p_c} [40]. We use c to denote the label of topologically distinct phases. Our proposed clustering algorithm is similar to the hierarchical clustering based on neighbor relations [57,58]. Given any new H_j , we can quickly identify its phase by comparing it with the samples in \mathcal{S} : it is topologically equivalent to H_{p_c} if $\mathcal{K}_{p_c,j} < \kappa_c$ and $H_{p_c} \in \mathcal{S}$, and otherwise it represents a new phase.

Firstly, we verify our approach in some well-known topological insulating models. Figure 2(a) shows a 1D Su-Schrieffer-Heeger (SSH) chain with long-range hopping under chiral symmetry [40], a 2D Chern insulator of Haldane model [1,59], and a higher-order topological insulator (HOTI) in a Kagome lattice [60,61]. After generating 500 samples of each model with random

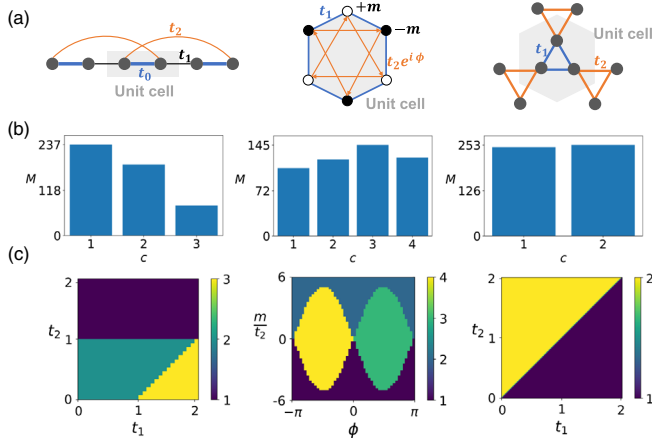


FIG. 2. Demonstration of unsupervised learning of topological classifications and topological phase diagrams. (a) The three models, the 1D SSH model with long-range hopping, Haldane model, and HOTI in Kagome lattice, have been demonstrated. Here, we set $t_0 = 1$, $t_1, t_2 \in [0, 2]$ for the 1D SSH model with long-range hopping, $t_1 = 1$, $t_2 = 0.1$, $m \in [-6t_2, 6t_2]$, and $\phi \in [-\pi, \pi]$ for the Haldane model, $t_1, t_2 \in [0, 1]$ for HOTI in Kagome lattice. (b) The number of samples M for the topologically different phases. The values of c denote the labels of topological different phases. (c) The topological phase diagrams can be obtained based on the similarity between the Hamiltonian with the given parameters and Hamiltonians in \mathcal{S} . The different colors and labels denote the topologically different phases but not the topological invariants.

parameters, we calculate their similarities and perform the clustering algorithm to obtain the number of phases [40]. We can see from Fig. 2(b) that the number of topologically distinct phases, denoted as N_c , is as follows: $N_c = 3$ for the 1D model, $N_c = 4$ for the 2D Chern insulator, and $N_c = 2$ for the HOTI. After labeling all phases (i.e., with different values of c), we can calculate their similarities with the samples and classify samples with the label of the sample H_{p_c} which has the maximum similarity. Consequently, we can obtain the topological phase diagrams unsupervisedly, as shown in Fig. 2(c) [40]. In particular, in the 2D Haldane model, our algorithm can not only capture the parameter regions with a nonzero Chern number, but also identify the regions that are described by valley Chern numbers (or within the methodology of topological quantum chemistry [62] and symmetry indicators [63]). All classification results are in excellent agreement with the corresponding topological invariants [40]. The unsupervised classification of fragile topology [64,65], Hopf insulator [66], and delicate topology [67] can be found in the Supplemental Material [40].

In the following, we proceed to achieve the topological classification of general gapped Hamiltonians in different symmetry classes. Firstly, we demonstrate unsupervised classification of zero-dimensional (0D) topological systems. We follow the same symmetry class definition as the Altland-Zirnbauer (AZ) classes [9], which denote ten symmetry classes of topological insulators and superconductors according to the time-reversal (\mathcal{T}), particle-hole (\mathcal{P}), and chiral (\mathcal{C}) symmetries. Here, we choose the representations of symmetry operators in the basis of Ref. [68] and exploit the random matrix technologies to generate the 0D $n \times n$ Hamiltonians under different symmetries [40,69]. We generate 500 samples for each symmetry class, calculate their similarities based on Eq. (1), and then perform the cluster algorithm to obtain N_c and $\{M_c\}$. The numbers of samples classified into different phases for each symmetry class in the 0D system are plotted in Fig. 3. We can see that there are $N_c = n + 1$ phases for the classes A and AI, and $N_c = n/2 + 1$ phases for the class AII [40], which correspond to the topological classification \mathbb{Z} and $2\mathbb{Z}$, respectively. There are only $N_c = 2$ phases for the classes BDI and D, meaning that they belong to \mathbb{Z}_2 . The remaining classes have only $N_c = 1$ phase, corresponding to the trivial group. These data-driven classifications are in good agreement with the theoretical predictions based on homotopy group of classifying spaces or K theory for Hamiltonians with infinite bands [5,6,9]. In particular, our method requires no *a priori* knowledge of topological invariants and is universal for different symmetry conditions.

For higher dimensions, we exploit the dimension increment method in Refs. [40,70]. After generating 500 samples of 1D, 2D, and 3D Hamiltonians [40,70], respectively, we perform our cluster algorithm with similarities of

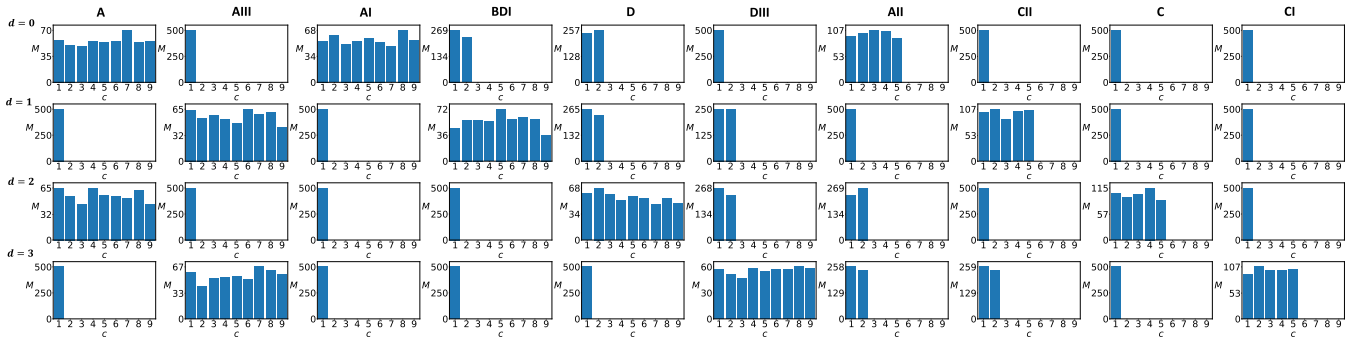


FIG. 3. Classifications of Hamiltonians in different symmetry classes from 0D to 3D. The symmetry labels (black bold font on the top) are the symmetry classes in terms of AZ classes. We generate Hamiltonians with dimensions ranging from 1D to 3D based on the 0D $n \times n$ Hamiltonians [40]. Obviously, it is \mathbb{Z} when the number of phases is equal to $N_c = n + 1$, $2\mathbb{Z}$ when the number of phases is equal to $N_c = n/2 + 1$, \mathbb{Z}_2 for the constant number of phases 2 ($N_c = 2$), and trivial for only 1 phase ($N_c = 1$). Here, we set $n = 8$; d denotes the dimension.

Eq. (1) and obtain the classification results of these topological Hamiltonians in Fig. 3. One can see that the translation symmetry from increasing dimensions can affect the topological classifications. We perform clustering for all symmetry classes of random d -dimensional Hamiltonians from $d = 0$ to $d = 9$ [40], and the number of phases for different dimensions has been concluded in Table I. The numbers of phases $n + 1$, $n/2 + 1$, 2, and 1 correspond to \mathbb{Z} , $2\mathbb{Z}$, \mathbb{Z}_2 , and the trivial group, respectively. From Fig. 3 and Table I, we can see that the numbers of topologically distinct phases have obvious periodic patterns when the dimension increases $d \rightarrow d + 1$: (1) The numbers of phases exchange between A and AIII: $n + 1 \Leftrightarrow 1$; (2) The classification pattern “shifts” horizontally by one symmetry class. Theoretically, this principle of periodicity is termed as Bott periodicity [5,6]. Besides Bott periodicity, we also show that the number of topologically distinct phases is affected by the number of bands [40], e.g., $N_c = n + 1$ for the 1D AIII class, $N_c = n/2 + 1$ for the 2D C class. These relations have not been revealed in the previous theories due to the assumption of infinite bands. It should be mentioned that we consider nearest-neighbor hopping in the unsupervised learning in Fig. 3 and Table I, because the

topological invariants can be fully accessed by increasing the number of bands, whose effect is similar (or equivalent) to introducing long-range hopping. The discussion about the effect of long-range hopping on topological classification can be found in Supplemental Material [40].

Besides the global symmetries (i.e., \mathcal{P} , \mathcal{T} , and \mathcal{C}), spatial symmetry can also play an important role in topological phases [71–75]. For example, the 2D spinless insulator in the AI class is trivial if only under time-reversal symmetry \mathcal{T} . However, after introducing spatial symmetry, the insulator in the AI class can be topological, e.g., in the higher-order topological insulator [11,60,61]. Since the family of spatial symmetries is quite large, here we focus on the topological classification of C_3 and C_4 -symmetric 2D lattices with time-reversal symmetry (i.e., wallpaper symmetry groups $p3$ and $p4$, respectively). We assume that there are three sites in the unit cell of a C_3 -symmetric 2D lattice and four sites in a C_4 -symmetric 2D lattice, corresponding to the Wyckoff positions $3d$ and $4d$, respectively, as shown in Fig. 4. We further assume that there is one electron in the unit cell of the C_3 -symmetric lattice and two electrons in the C_4 -symmetric lattice (i.e., half filling). We generate samples for each spatial symmetry, calculate

TABLE I. The number of topologically different phases N_c for the d -dimensional Hamiltonians in different symmetry classes. Here, we generate the higher-dimensional Hamiltonians based on the 0D $n \times n$ random Hamiltonians [40].

d	A	AIII	AI	BDI	D	DIII	AII	CII	C	CI
0	$n + 1$	1	$n + 1$	2	2	1	$n/2 + 1$	1	1	1
1	1	$n + 1$	1	$n + 1$	2	2	1	$n/2 + 1$	1	1
2	$n + 1$	1	1	1	$n + 1$	2	2	1	$n/2 + 1$	1
3	1	$n + 1$	1	1	1	$n + 1$	2	2	1	$n/2 + 1$
4	$n + 1$	1	$n/2 + 1$	1	1	1	$n + 1$	2	2	1
5	1	$n + 1$	1	$n/2 + 1$	1	1	1	$n + 1$	2	2
6	$n + 1$	1	2	1	$n/2 + 1$	1	1	1	$n + 1$	2
7	1	$n + 1$	2	2	1	$n/2 + 1$	1	1	1	$n + 1$
8	$n + 1$	1	$n + 1$	2	2	1	$n/2 + 1$	1	1	1
9	1	$n + 1$	1	$n + 1$	2	2	1	$n/2 + 1$	1	1

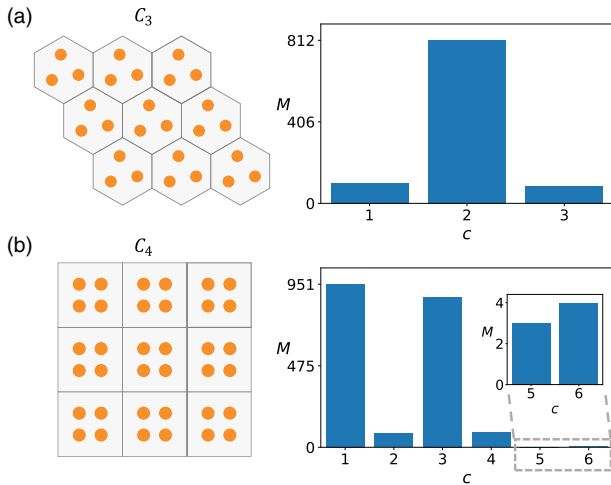


FIG. 4. Topological classifications of 2D spinless lattice with spatial symmetries C_3 and C_4 . (a) The C_3 -symmetric lattice. There are three sites in the unit cell, corresponding to the Wyckoff positions $3d$ for the wallpaper group $p3$. There are $N_c = 3$ topologically different phases. Here, c denotes the class of phases and M denotes the number of samples in topologically different phases. The values of M for each c are 102, 812, and 86, respectively. (b) The C_4 -symmetric lattice. There are four sites in the unit cell, corresponding to the Wyckoff position $4d$ for the wallpaper group $p4$. There are $N_c = 6$ different phases. The values of M for each c are 951, 81, 875, 86, 3, and 4, respectively. Here, we generate 1000 samples for C_3 symmetry and 2000 samples for C_4 symmetry.

their similarities based on Eq. (1), and then perform the cluster algorithm to obtain N_c and $\{M_c\}$ [40]. The plots for the numbers of samples in different phases for each spatial symmetry have been shown in Fig. 4. From the results, we can see that there are $N_c = 3$ topologically distinct phases for C_3 symmetry, and $N_c = 6$ for C_4 symmetry. In contrast to the traditional theoretical approach [71,73,76–78], our data-driven identification of topological phases does not require the definition of a time-reversal topological invariant. More details can be found in the Supplemental Material [40].

To summarize, we propose the unsupervised learning of topological classification and the data-driven construction of the topological periodic table. Our method is based on an efficient similarity function to accurately measure topological differences between Hamiltonians and a cluster algorithm for detecting the number of clusters automatically. We demonstrate the validity of our algorithm for classifying topological phases accurately and finding phase diagrams without human knowledge *a priori* or concepts of topological invariants. Our approach can be extended to classify the Hamiltonians under the other symmetries [79], i.e., projective symmetry [80–82], non-Hermitian symmetry [39,83], and non-Abelian symmetry [84–86]. Our Letter not only paves the way toward unsupervised data-driven topological classification, but also measures

a significant step in the early stage of machine learning application in fundamental physics.

This research is supported by Singapore National Research Foundation Competitive Research Program Grant No. NRF-CRP23-2019-0007, Singapore Ministry of Education Academic Research Fund Tier 3 Grant No. MOE2016-T3-1-006, and Tier 2 Grant No. MOE2019-T2-2-085.

*Corresponding author.

blzhang@ntu.edu.sg

- [1] F. D. M. Haldane, Nobel lecture: Topological quantum matter, *Rev. Mod. Phys.* **89**, 040502 (2017).
- [2] D. Xiao, M.-C. Chang, and Q. Niu, Berry phase effects on electronic properties, *Rev. Mod. Phys.* **82**, 1959 (2010).
- [3] M. Z. Hasan and C. L. Kane, Colloquium: Topological insulators, *Rev. Mod. Phys.* **82**, 3045 (2010).
- [4] X.-L. Qi and S.-C. Zhang, Topological insulators and superconductors, *Rev. Mod. Phys.* **83**, 1057 (2011).
- [5] C.-K. Chiu, J. C. Teo, A. P. Schnyder, and S. Ryu, Classification of topological quantum matter with symmetries, *Rev. Mod. Phys.* **88**, 035005 (2016).
- [6] A. Kitaev, V. Lebedev, and M. Feigel'man, Periodic table for topological insulators and superconductors, *AIP Conf. Proc.* **1134**, 22 (2009).
- [7] A. P. Schnyder, S. Ryu, A. Furusaki, A. W. W. Ludwig, V. Lebedev, and M. Feigel'man, Classification of topological insulators and superconductors, *AIP Conf. Proc.* **1134**, 10 (2009).
- [8] A. Bansil, H. Lin, and T. Das, Colloquium: Topological band theory, *Rev. Mod. Phys.* **88**, 021004 (2016).
- [9] A. Altland and M. R. Zirnbauer, Nonstandard symmetry classes in mesoscopic normal-superconducting hybrid structures, *Phys. Rev. B* **55**, 1142 (1997).
- [10] F. Zhang, A. H. MacDonald, and E. J. Mele, Valley chern numbers and boundary modes in gapped bilayer graphene, *Proc. Natl. Acad. Sci. U.S.A.* **110**, 10546 (2013).
- [11] W. A. Benalcazar, B. A. Bernevig, and T. L. Hughes, Quantized electric multipole insulators, *Science* **357**, 61 (2017).
- [12] G. Carleo, I. Cirac, K. Cranmer, L. Daudet, M. Schuld, N. Tishby, L. Vogt-Maranto, and L. Zdeborová, Machine learning and the physical sciences, *Rev. Mod. Phys.* **91**, 045002 (2019).
- [13] P. Mehta, M. Bukov, C.-H. Wang, A. G. Day, C. Richardson, C. K. Fisher, and D. J. Schwab, A high-bias, low-variance introduction to machine learning for physicists, *Phys. Rep.* **810**, 1 (2019).
- [14] V. Dunjko and H. J. Briegel, Machine learning & artificial intelligence in the quantum domain: A review of recent progress, *Rep. Prog. Phys.* **81**, 074001 (2018).
- [15] E. P. L. van Nieuwenburg, Y.-H. Liu, and S. D. Huber, Learning phase transitions by confusion, *Nat. Phys.* **13**, 435 (2017).
- [16] G. Carleo and M. Troyer, Solving the quantum many-body problem with artificial neural networks, *Science* **355**, 602 (2017).

- [17] J. Venderley, V. Khemani, and E.-A. Kim, Machine Learning Out-of-Equilibrium Phases of Matter, *Phys. Rev. Lett.* **120**, 257204 (2018).
- [18] H. Wang, Y. Rivenson, Y. Jin, Z. Wei, R. Gao, H. Gnaudin, L. A. Bentolila, C. Kural, and A. Ozcan, Deep learning enables cross-modality super-resolution in fluorescence microscopy, *Nat. Methods* **16**, 103 (2019).
- [19] L. Fang, F. Monroe, S. W. Novak, L. Kirk, C. R. Schiavon, S. B. Yu, T. Zhang, M. Wu, K. Kastner, A. A. Latif, Z. Lin, A. Shaw, Y. Kubota, J. Mendenhall, Z. Zhang, G. Pekkurnaz, K. Harris, J. Howard, and U. Manor, Deep learning-based point-scanning super-resolution imaging, *Nat. Methods* **18**, 406 (2021).
- [20] C. Zhu, E. A. Chan, Y. Wang, W. Peng, R. Guo, B. Zhang, C. Soci, and Y. Chong, Image reconstruction through a multimode fiber with a simple neural network architecture, *Sci. Rep.* **11**, 896 (2021).
- [21] C. Qian, B. Zheng, Y. Shen, L. Jing, E. Li, L. Shen, and H. Chen, Deep-learning-enabled self-adaptive microwave cloak without human intervention, *Nat. Photonics* **14**, 383 (2020).
- [22] W. Ma, Z. Liu, Z. A. Kudyshev, A. Boltasseva, W. Cai, and Y. Liu, Deep learning for the design of photonic structures, *Nat. Photonics* **15**, 77 (2021).
- [23] L. Li, H. Ruan, C. Liu, Y. Li, Y. Shuang, A. Alù, C.-W. Qiu, and T. J. Cui, Machine-learning reprogrammable metasurface imager, *Nat. Commun.* **10**, 1082 (2019).
- [24] Y. Li, Y. Xu, M. Jiang, B. Li, T. Han, C. Chi, F. Lin, B. Shen, X. Zhu, L. Lai, and Z. Fang, Self-Learning Perfect Optical Chirality via a Deep Neural Network, *Phys. Rev. Lett.* **123**, 213902 (2019).
- [25] Z. Liu, D. Zhu, S. P. Rodrigues, K.-T. Lee, and W. Cai, Generative model for the inverse design of metasurfaces, *Nano Lett.* **18**, 6570 (2018).
- [26] W. Ma, F. Cheng, and Y. Liu, Deep-learning-enabled on-demand design of chiral metamaterials, *ACS Nano* **12**, 6326 (2018).
- [27] D. Liu, Y. Tan, E. Khoram, and Z. Yu, Training deep neural networks for the inverse design of nanophotonic structures, *ACS Photonics* **5**, 1365 (2018).
- [28] Y. Long, J. Ren, Y. Li, and H. Chen, Inverse design of photonic topological state via machine learning, *Appl. Phys. Lett.* **114**, 181105 (2019).
- [29] L. Pilozzi, F. A. Farrelly, G. Marcucci, and C. Conti, Machine learning inverse problem for topological photonics, *Commun. Phys.* **1**, 57 (2018).
- [30] V. Peano, F. Sapper, and F. Marquardt, Rapid Exploration of Topological Band Structures Using Deep Learning, *Phys. Rev. X* **11**, 021052 (2021).
- [31] L. Wang, Discovering phase transitions with unsupervised learning, *Phys. Rev. B* **94**, 195105 (2016).
- [32] S. J. Wetzel, Unsupervised learning of phase transitions: From principal component analysis to variational autoencoders, *Phys. Rev. E* **96**, 022140 (2017).
- [33] J. F. Rodriguez-Nieva and M. S. Scheurer, Identifying topological order through unsupervised machine learning, *Nat. Phys.* **15**, 790 (2019).
- [34] Y. Long, J. Ren, and H. Chen, Unsupervised Manifold Clustering of Topological Phononics, *Phys. Rev. Lett.* **124**, 185501 (2020).
- [35] M. S. Scheurer and R.-J. Slager, Unsupervised Machine Learning and Band Topology, *Phys. Rev. Lett.* **124**, 226401 (2020).
- [36] Y. Che, C. Gneiting, T. Liu, and F. Nori, Topological quantum phase transitions retrieved through unsupervised machine learning, *Phys. Rev. B* **102**, 134213 (2020).
- [37] O. Balabanov and M. Granath, Unsupervised learning using topological data augmentation, *Phys. Rev. Res.* **2**, 013354 (2020).
- [38] S. Park, Y. Hwang, and B.-J. Yang, Unsupervised learning of topological phase diagram using topological data analysis, *Phys. Rev. B* **105**, 195115 (2022).
- [39] L.-W. Yu and D.-L. Deng, Unsupervised Learning of Non-Hermitian Topological Phases, *Phys. Rev. Lett.* **126**, 240402 (2021).
- [40] See Supplemental Material at <http://link.aps.org/supplemental/10.1103/PhysRevLett.130.036601> for more details about the random Hamiltonian generation, the unsupervised classifications of the well-known topological models, the Hamiltonian in the $d \geq 4$ dimension, the Hamiltonian with long-range hopping, and unsupervised classifications of Hamiltonians under spatial symmetries, which include the Ref. [41–50].
- [41] R. R. Coifman, S. Lafon, A. B. Lee, M. Maggioni, B. Nadler, F. Warner, and S. W. Zucker, Geometric diffusions as a tool for harmonic analysis and structure definition of data: Diffusion maps, *Proc. Natl. Acad. Sci. U.S.A.* **102**, 7426 (2005).
- [42] W. P. Su, J. R. Schrieffer, and A. J. Heeger, Solitons in Polyacetylene, *Phys. Rev. Lett.* **42**, 1698 (1979).
- [43] J. Lu, C. Qiu, L. Ye, X. Fan, M. Ke, F. Zhang, and Z. Liu, Observation of topological valley transport of sound in sonic crystals, *Nat. Phys.* **13**, 369 (2017).
- [44] M. Ezawa, Higher-Order Topological Insulators and Semimetals on the Breathing Kagome and Pyrochlore Lattices, *Phys. Rev. Lett.* **120**, 026801 (2018).
- [45] M. Serra-Garcia, V. Peri, R. Ssstrunk, O. R. Bilal, T. Larsen, L. G. Villanueva, and S. D. Huber, Observation of a phononic quadrupole topological insulator, *Nature (London)* **555**, 342 (2018).
- [46] B. A. Bernevig, T. L. Hughes, and S.-C. Zhang, Quantum spin hall effect and topological phase transition in HgTe quantum wells, *Science* **314**, 1757 (2006).
- [47] C.-X. Liu, X.-L. Qi, H. Zhang, X. Dai, Z. Fang, and S.-C. Zhang, Model hamiltonian for topological insulators, *Phys. Rev. B* **82**, 045122 (2010).
- [48] J. K. Asbóth and H. Obuse, Bulk-boundary correspondence for chiral symmetric quantum walks, *Phys. Rev. B* **88**, 121406(R) (2013).
- [49] M. Maffei, A. Dauphin, F. Cardano, M. Lewenstein, and P. Massignan, Topological characterization of chiral models through their long time dynamics, *New J. Phys.* **20**, 013023 (2018).
- [50] S. A. Skirlo, L. Lu, Y. Igarashi, Q. Yan, J. Joannopoulos, and M. Soljačić, Experimental Observation of Large Chern Numbers in Photonic Crystals, *Phys. Rev. Lett.* **115**, 253901 (2015).
- [51] M. Ezawa, Y. Tanaka, and N. Nagaosa, Topological phase transition without gap closing, *Sci. Rep.* **3**, 2790 (2013).

- [52] Y. Yang, H. Li, L. Sheng, R. Shen, D. N. Sheng, and D. Y. Xing, Topological phase transitions with and without energy gap closing, *New J. Phys.* **15**, 083042 (2013).
- [53] A. Kitaev, Anyons in an exactly solved model and beyond, *Ann. Phys. (Amsterdam)* **321**, 2 (2006).
- [54] G.-G. Liu, Y. Yang, X. Ren, H. Xue, X. Lin, Y.-H. Hu, H. xiang Sun, B. Peng, P. Zhou, Y. Chong, and B. Zhang, Topological Anderson Insulator in Disordered Photonic Crystals, *Phys. Rev. Lett.* **125**, 133603 (2020).
- [55] N. P. Mitchell, L. M. Nash, D. Hexner, A. M. Turner, and W. T. M. Irvine, Amorphous topological insulators constructed from random point sets, *Nat. Phys.* **14**, 380 (2018).
- [56] S. Ryu, A. P. Schnyder, A. Furusaki, and A. W. W. Ludwig, Topological insulators and superconductors: Tenfold way and dimensional hierarchy, *New J. Phys.* **12**, 065010 (2010).
- [57] M. Saquib Sarfraz, V. Sharma, and R. Stiefelhagen, Efficient parameter-free clustering using first neighbor relations, [arXiv:1902.11266](https://arxiv.org/abs/1902.11266).
- [58] X. Wei, Q. Yang, Y. Gong, N. Ahuja, and M.-H. Yang, Superpixel hierarchy, *IEEE Trans. Image Process.* **27**, 4838 (2018).
- [59] F. D. M. Haldane, Model for a Quantum Hall Effect Without Landau Levels: Condensed-Matter Realization of the “Parity Anomaly”, *Phys. Rev. Lett.* **61**, 2015 (1988).
- [60] H. Xue, Y. Yang, F. Gao, Y. Chong, and B. Zhang, Acoustic higher-order topological insulator on a kagome lattice, *Nat. Mater.* **18**, 108 (2019).
- [61] X. Ni, M. Weiner, A. Alù, and A. B. Khanikaev, Observation of higher-order topological acoustic states protected by generalized chiral symmetry, *Nat. Mater.* **18**, 113 (2019).
- [62] B. Bradlyn, L. Elcoro, J. Cano, M. G. Vergniory, Z. Wang, C. Felser, M. I. Aroyo, and B. A. Bernevig, Topological quantum chemistry, *Nature (London)* **547**, 298 (2017).
- [63] H. C. Po, A. Vishwanath, and H. Watanabe, Symmetry-based indicators of band topology in the 230 space groups, *Nat. Commun.* **8**, 50 (2017).
- [64] Z.-D. Song, L. Elcoro, and B. A. Bernevig, Twisted bulk-boundary correspondence of fragile topology, *Science* **367**, 794 (2020).
- [65] V. Peri, Z.-D. Song, M. Serra-Garcia, P. Engeler, R. Queiroz, X. Huang, W. Deng, Z. Liu, B. A. Bernevig, and S. D. Huber, Experimental characterization of fragile topology in an acoustic metamaterial, *Science* **367**, 797 (2020).
- [66] J. E. Moore, Y. Ran, and X.-G. Wen, Topological Surface States in Three-Dimensional Magnetic Insulators, *Phys. Rev. Lett.* **101**, 186805 (2008).
- [67] A. Nelson, T. Neupert, A. Alexandradinata, and T. Bzdušek, Delicate topology protected by rotation symmetry: Crystalline hopf insulators and beyond, *Phys. Rev. B* **106**, 075124 (2022).
- [68] I. C. Fulga, F. Hassler, and A. R. Akhmerov, Scattering theory of topological insulators and superconductors, *Phys. Rev. B* **85**, 165409 (2012).
- [69] F. Mezzadri, How to generate random matrices from the classical compact groups, [arXiv:math-ph/0609050](https://arxiv.org/abs/math-ph/0609050).
- [70] J. C. Y. Teo and C. L. Kane, Topological defects and gapless modes in insulators and superconductors, *Phys. Rev. B* **82**, 115120 (2010).
- [71] L. Fu, Topological Crystalline Insulators, *Phys. Rev. Lett.* **106**, 106802 (2011).
- [72] Y. Tanaka, Z. Ren, T. Sato, K. Nakayama, S. Souma, T. Takahashi, K. Segawa, and Y. Ando, Experimental realization of a topological crystalline insulator in SnTe, *Nat. Phys.* **8**, 800 (2012).
- [73] Y. Ando and L. Fu, Topological crystalline insulators and topological superconductors: From concepts to materials, *Annu. Rev. Condens. Matter Phys.* **6**, 361 (2015).
- [74] Y. Okada, M. Serbyn, H. Lin, D. Walkup, W. Zhou, C. Dhital, M. Neupane, S. Xu, Y. J. Wang, R. Sankar, F. Chou, A. Bansil, M. Z. Hasan, S. D. Wilson, L. Fu, and V. Madhavan, Observation of dirac node formation and mass acquisition in a topological crystalline insulator, *Science* **341**, 1496 (2013).
- [75] Y. Liu, S. Leung, F.-F. Li, Z.-K. Lin, X. Tao, Y. Poo, and J.-H. Jiang, Bulk–disclination correspondence in topological crystalline insulators, *Nature (London)* **589**, 381 (2021).
- [76] L. Fu and C. L. Kane, Topological insulators with inversion symmetry, *Phys. Rev. B* **76**, 045302 (2007).
- [77] Y. Tanaka, R. Takahashi, T. Zhang, and S. Murakami, Theory of inversion- \mathbb{Z}_4 protected topological chiral hinge states and its applications to layered antiferromagnets, *Phys. Rev. Res.* **2**, 043274 (2020).
- [78] W. A. Benalcazar, T. Li, and T. L. Hughes, Quantization of fractional corner charge in \mathbb{C}_n -symmetric higher-order topological crystalline insulators, *Phys. Rev. B* **99**, 245151 (2019).
- [79] R. Li, J. Wang, X.-L. Qi, and S.-C. Zhang, Dynamical axion field in topological magnetic insulators, *Nat. Phys.* **6**, 284 (2010).
- [80] Y. X. Zhao, Y.-X. Huang, and S. A. Yang, \mathbb{Z}_2 -projective translational symmetry protected topological phases, *Phys. Rev. B* **102**, 161117(R) (2020).
- [81] H. Xue, Z. Wang, Y.-X. Huang, Z. Cheng, L. Yu, Y. Foo, Y. Zhao, S. A. Yang, and B. Zhang, Projectively Enriched Symmetry and Topology in Acoustic Crystals, *Phys. Rev. Lett.* **128**, 116802 (2022).
- [82] T. Li, J. Du, Q. Zhang, Y. Li, X. Fan, F. Zhang, and C. Qiu, Acoustic Mbius Insulators from Projective Symmetry, *Phys. Rev. Lett.* **128**, 116803 (2022).
- [83] K. Kawabata, K. Shiozaki, M. Ueda, and M. Sato, Symmetry and Topology in Non-Hermitian Physics, *Phys. Rev. X* **9**, 041015 (2019).
- [84] Q. Guo, T. Jiang, R.-Y. Zhang, L. Zhang, Z.-Q. Zhang, B. Yang, S. Zhang, and C. T. Chan, Experimental observation of non-Abelian topological charges and edge states, *Nature (London)* **594**, 195 (2021).
- [85] E. Yang, B. Yang, O. You, H.-C. Chan, P. Mao, Q. Guo, S. Ma, L. Xia, D. Fan, Y. Xiang, and S. Zhang, Observation of Non-Abelian Nodal Links in Photonics, *Phys. Rev. Lett.* **125**, 033901 (2020).
- [86] Q. Wu, A. A. Soluyanov, and T. Bzdušek, Non-Abelian band topology in noninteracting metals, *Science* **365**, 1273 (2019).